Fabrication of Highly Ordered TiO_2 Nanotube Arrays Using an Organic Electrolyte

Chuanmin Ruan, Maggie Paulose, Oomman K. Varghese, Gopal K. Mor, and Craig A. Grimes*

Department of Electrical Engineering and Department of Materials Science and Engineering, 217 Materials Research Laboratory, The Pennsylvania State University, University Park, Pennsylvania 16802

Received: May 24, 2005; In Final Form: June 24, 2005

Anodization of titanium in a fluorinated dimethyl sulfoxide (DMSO) and ethanol mixture electrolyte is investigated. The prepared anodic film has a highly ordered nanotube-array surface architecture. Using a 20 V anodization potential (vs Pt) nanotube arrays having an inner diameter of 60 nm and 40 nm wall thickness are formed. The overall length of the nanotube arrays is controlled by the duration of the anodization, with nanotubes appearing only after approximately 48 h; a 72 h anodization results in a nanotube array approximately 2.3 μm in length. The photoelectrochemical response of the nanotube-array photoelectrodes is studied using a 1 M KOH solution under both UV and visible (AM 1.5) illumination. Enhanced photocurrent density is observed for samples obtained in the organic electrolyte, with an UV photoconversion efficiency of 10.7%.

Introduction

Over the past several years specific TiO_2 nanostructures have become a focus of considerable interest as they possess unique properties relevant to applications including chemical sensing,[1] photocatalysis,[2] and photovoltaics.[3] Several fabrication routes including anodic oxidation,[4,5] electrochemical lithography,[6] photoelectrochemical etching,[7] sol−gel,[8] hydrothermal synthesis,[9−11] and template synthesis[12,13] have been used to prepare nanometer-sized TiO_2. tubules, wires, dots, and pillars. Among these methods for preparing of TiO_2 nanostructures, electrochemical anodization of titanium in fluorinated electrolytes is a relatively simple process to engineer highly ordered TiO_2 porous or tubular structures. In the anodization of titanium electrolyte composition is a critical determinant with regard to the resulting surface morphologies, and hence properties of the anodic film. Several aqueous electrolytes such as HF/H_2O,[4] $HF/H_2SO_4/H_2O$,[14] $HF-CrO_4/H_2O$,[15] and $KF/NaF/H_2O$[16] have recently been used to create TiO_2 nanostructures.

Various organic solvents have been used in the anodic fabrication of macroporous silicon and aluminum oxide.[17−20] It has been shown that organic solvents essentially suppress the electrochemical oxidation of Si in comparison to an aqueous electrolyte[17,18] and that organic solvents can act as mild oxidizing reactants for silicon.[21] We hypothesize new types of anodic titania films with salient characteristics could be obtained by anodizing titanium in various organic electrolytes. However, to the best of our knowledge, no study on electrochemical etching of titanium to prepare highly ordered TiO_2 nanotube arrays in organic solvents has been reported. As previously reported in the anodic fabrication of nanoporous alumina using a neutral organic electrolyte,[22] we hypothesize that a significant amount of organic material could be incorporated into anodic TiO_2 films by using organic electrolytes. Such in-situ chemical doping of the TiO_2-nanotube arrays might prove useful in, for example, band gap engineering of the resulting material or, with respect to use as gas sensors, modifying the materials response to specific chemicals.

* To whom correspondence should be addressed. E-mail: cgrimes@engr.psu.edu.

In this work we examine the electrochemical etching of titanium under potentiostatic conditions in fluorinated 1:1 dimethyl sulfoxide (DSMO) and ethanol, varying a range of anodizing conditions to achieve highly ordered TiO_2 nanotube arrays. The crystallographic structure and chemical composition of the resulting anodic films are investigated by glancing angle X-ray diffraction and X-ray photoelectron spectroscopy. The photoelectrochemical properties of the films are examined in 1 mol/L KOH solution upon illumination of UV ($<$400 nm) and simulated sunlight (AM 1.5). Our results show that use of an organic electrolyte results in a unique TiO_2 nanomorphology having enhanced photoelectrochemical properties.

Experimental Section

Titanium sheets (0.25 mm thick, 99.7% purity), hydrofluoric acid (48%), DMSO (99.6%), and ethyl alcohol (99.9%) were purchased from Aldrich Corp. (Milwaukee, WI). Titanium samples were degreased by sonicating in acetone, ethanol, and DI water, followed by rinsing with DI water and drying in a nitrogen stream. Electrochemical anodization of titanium was carried out using a DC power supply (Agilent Technologies, 0−60 V) connected with a multimeter (Keithley 2000) interfaced to a computer. All anodization experiments were carried out at room temperature using a two-electrode system (2 cm separation). Anodic films were grown from titanium by potentiostatic anodization in an organic electrolyte containing 4% HF (standard 48% aqueous HF) using a platinum foil counter electrode. After fabrication, the samples required washing in a dilute HF and water solution to remove precipitation atop the nanotube layers. The obtained highly ordered titania nanotube arrays, initially amorphous, were crystallized by annealing in an oxygen atmosphere for 6 h at 550 °C with heating and cooling rates of 1°C/min.

The morphologies of the titania nanotubes were studied using a JSM-6700 field emission scanning electron microscope (FESEM) from JEOL (Peabody, MA). A glancing angle X-ray diffractometer (GAXRD) from Philips (model X'pert MRD PRO), The Netherlands, was used to determine the crystalline structure of the annealed samples. The surface chemical composition of samples was analyzed by X-ray photoelectron

10.1021/jp052736u CCC: $30.25
Published on Web 07/29/2005

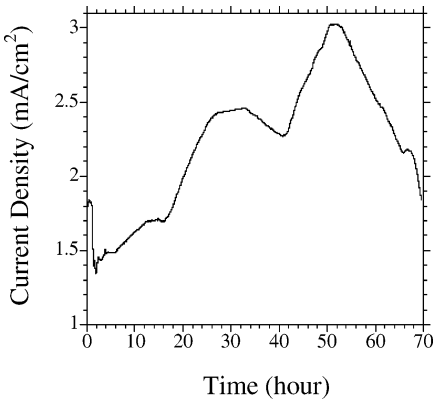

Figure 1. Typical potentiostatic current−time response for a titanium foil electrode in DSMO and ethanol mixture solution (1:1) containing 4% HF at +20 V (vs Pt) at room temperature.

spectroscopy (XPS) from Kratos Analytical Axis Ultra. Monochromatic aluminum (1486.6 eV) was used as the X-ray source (280 W). All binding energies were calibrated to C−C C1s peak at 285 eV of the surface adventitious carbon.

Photoelectrochemical measurements were performed using a CHI electrochemical analyzer (CH instruments, Dallas, TX) in a standard three- electrode configuration with a platinum plate counter electrode, a saturated Ag/AgCl reference electrode and TiO_2 nanotube-array (photoanode) working electrode. Electrical contact was taken from the backside of the Ti foil after removing the oxide layer by mechanical scribing; an electrically insulated copper wire was attached on the backside using conductive silver−epoxy adhesive. The backside of the sample was fixed to a glass substrate using a nonconductive epoxy, which also covered the edges of the foil to ensure an electrode exposure area of 1 cm^2. A 50 W metal hydride lamp (EXFO Lite) was used as the UV light source. The light was passed through broadband optical filters, which allowed only wavelengths between 320 and 400 nm to be incident on the TiO_2 photoanode at a measured intensity of 96 mW/cm^2. For visible spectrum testing, a sun light simulator, AM 1.5, provided a light intensity of 100 mW/cm^2.

Results and Discussion

Potentiostatic Current Transient and Oxide Film Formation. Figure 1 shows a typical potentiostatic current density−time plot for a titanium electrode in 1:1 DMSO and ethanol solvent containing 4% HF at +20 V (vs Pt). The current density decreases during the first hour of anodization, indicating formation of a barrier layer on the titanium surface. Several peaks in the current density−time curve (Figure 1) can be observed over the 70 h period. The change in current density indicates changes in the titania film growth rate, structure, and real anodic area. Anodization of Ti in a HF containing organic solution involves several electrochemical and chemical reactions; electrochemical dissolution of metal titanium to ions of Ti, the oxidation of Ti^+ and/or Ti^{3+} to TiO_2, and localized dissolution of TiO_2 by hydrofluoric acid may occur simultaneously.

An increase in anodizing surface area may be attributed to the formation of the self-assembled porous structure on the titanium oxide surface.[23] The growth of this oxide layer is generally accompanied by the development of internal stresses,[24] the result of localized oxide etching by the fluoride. These stresses may be either tensile or compressive in nature, the magnitudes of which range from zero to values high enough to disrupt the film.[25] The sudden jumps in the current density

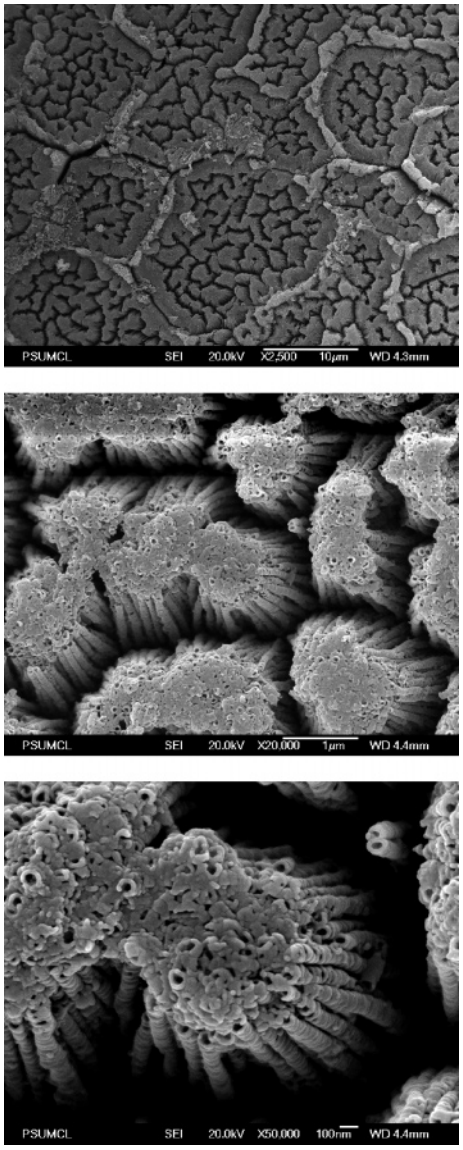

Figure 2. FE-SEM images of titanium foil sample anodized in DSMO and ethanol mixture solution (1:1) containing 4% HF at +20 V (vs Pt) for 70 h at room temperature. Surface is shown at three levels of magnification.

observed during anodization may be associated with these disruptions. It is worthy to note that in comparison with electrochemical etching of titanium in fluorinated aqueous solution the etching of titanium in fluorinated organic electrolyte is a relatively slow process. As previously reported,[26] at an anodization potential of +20 V titania undergoes an electric-field breakdown due to high current densities on the titanium foil at the beginning of anodization in an electrolyte of 2.5% HNO_3 plus 1% HF water solution. Hence, when using such aqueous electrolytes, the anodization potential must be slowly increased to obtain an anodic film. However, there is no need to apply a potential ramp while anodizing titanium in fluorinated organic electrolyte due to the high resistivity of the organic solvents. The resistivity for DMSO containing 4% HF is 14×10^3 Ω/cm.[27] At an anodization potential of +20 V the initial anodic current density is less than 2 mA/cm^2 (Figure 1). We note that after the initial potentiostatic response transient the current density−time behavior in both fluorinated aqueous and organic containing solutions are similar.[4]

Sample Morphology. FE-SEM images of a typical sample taken directly from the anodization bath are shown in Figure 2

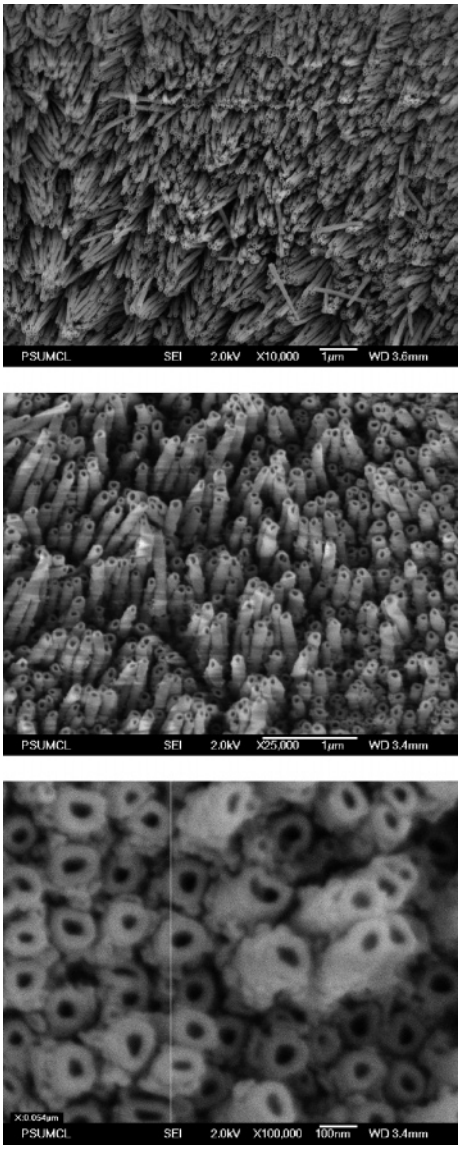

Figure 3. FE-SEM images of titanium foil sample anodized in DSMO and ethanol mixture solution (1:1) containing 4% HF at +20 V (vs Pt) for 70 h at room temperature, and prior to imaging washed in dilute HF. Surface is shown at three levels of magnification.

at varying degrees of magnification. The etching of this sample was performed in 1:1 DMSO and ethanol containing 4% HF at +20 V (vs Pt) for 70 h. The inhomogeneous cracked surface with cylindrical nanotubes piled together can be clearly observed. We believe the cracks are the result of surface stress originating during formation of the oxide films. Such cracks are not apparent in films fabricated by anodization of Ti in aqueous electrolytes, possibly due to the rapid oxide formation. We note that while nanotube arrays can be formed in aqueous electrolytes in less than 1 h,[4] in a 1:1 DMSO and ethanol electrolyte the well-organized nanotube-array structure can only be formed over a period of approximately 48 h.

FE-SEM images of a sample identical to that in Figure 2 that has been washed in dilute HF using ultrasonic agitation prior to imaging is shown in Figure 3. The surface coating partially obscuring the nanotube tops seen in Figure 2, which also acts to adhere the nanotubes together, has been removed. The obtained nanotubes have a pore size diameter of approximately 60 nm and a wall thickness of 40 nm. The FE-SEM cross-sectional view, Figure 4, indicates that the average

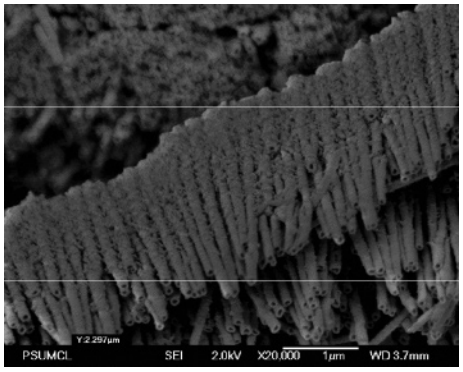

Figure 4. FE-SEM cross-sectional image of titanium foil sample anodized in DSMO and ethanol mixture solution (1:1) containing 4% HF at +20 V (vs Pt) for 70 h at room temperature.

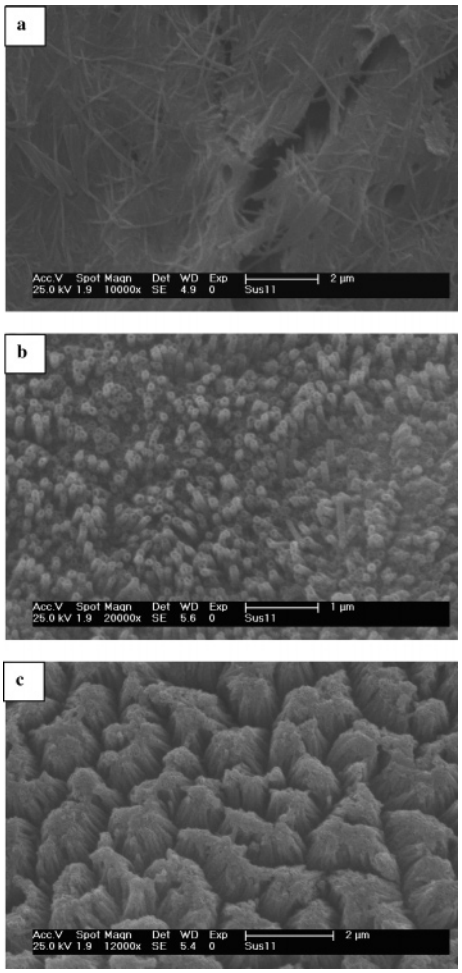

Figure 5. FE-SEM images of titanium anodized in DSMO and ethanol mixture solution (1:1) containing 4% HF at +20 V (vs Pt) for different etching time: **(a)** 24, **(b)** 48, and **(c)** 72 h.

height of the nanotubes is approximately 2.3 μm, with a variation of approximately 0.3 μm. The organic electrolyte nanotube arrays have pore sizes independent of the anodization time and proportional to the potential, similar to our findings for anodization in aqueous solutions.[16] The diameter of the resulting nanotubes at 10 V in 1:1 DMSO and ethanol containing 4% HF is $\approx$24 nm.

At the same applied potential the pore size of the nanotube arrays generated in the organic electrolyte is smaller than that obtained in aqueous electrolytes. For example, at an applied potential of 20 V the average nanotube pore diameter is

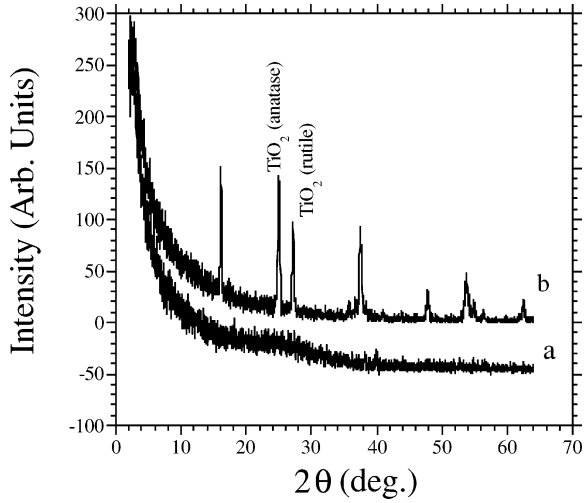

Figure 6. GAXRD patterns of titania nanotubes prepared by etching in DSMO and ethanol mixture solution (1:1) containing 4% HF at +10 V (vs Pt) for 70 h at room temperature: **(a)** as-fabricated sample; **(b)** same sample after being annealed at 550 °C.

TABLE 1: XPS Results of Titanium Etched in Fluorinated 1:1 DSMO and Ethanol at 20 V for 48 h, One of the Samples Annealed at 550 °C for 6 h

	atomic concn (%)					
	Ti	O	F	N	C	S
nanotubes	23.9	53.4	13.7	0.9	6.8	1.1
annealed nanotubes	26.6	64.3	1.6	0.5	5.8	1.2

approximately 100 nm in NaF/KF aqueous electrolytes[16] and only 60 nm in DMSO and ethanol electrolyte. Compared with the nanotube arrays fabricated in aqueous electrolytes, the nanotube arrays fabricated in the organic electrolytes are relatively fragile; the individual nanotubes of the array can be separated by sonication in dilute HF.

The evolution in surface morphology was studied as a function of anodization time. FE-SEM images of the samples etched for 24, 48, and 72 h in 1:1 DMSO and ethanol containing 4% HF at + 20 V (vs Pt) are shown in Figure 5a−c, respectively. It can be seen from Figure 5a that no self-organized pore or tubular structures are formed in the initial 24 h anodization. After 48 h a well-ordered nanotube-array structure is formed, Figure 5b. With the 72 h anodization the nanotubes clump, or lean together, presenting cracklike features readily apparent in the surface, Figure 5c.

Elemental and Structural Analysis. Figure 6 shows the GAXRD patterns of a typical sample obtained in 1:1 DMSO and ethanol containing 4% HF solution, as fabricated and after annealing at 550 °C for 6 h in an oxygen atmosphere with heating and cooling rates of 1°C/min. Results indicate that the as-fabricated nanotubes are amorphous. The annealed samples demonstrate a mixture of anatase and rutile, as indicated by curve b in Figure 6. Similar results are obtained for Ti anodized in aqueous electrolytes, indicating that the choice of electrolyte has no influence on the crystalline structure of resultant oxide films.

X-ray photoelectron spectroscopy (XPS) was used to determine the elemental composition of the nanotube samples, with results summarized in Table 1. The nanotube-array samples are predominately titanium and oxygen, with traces of fluorine and sulfur due to solvent incorporation in the anodic films. We believe surface contamination is the likely source for the nitrogen and carbon found in the samples. Chemical-state analysis for titanium indicates the sample is Ti^{4+} bonded with oxygen (TiO_2). Compared with sample fabricated in aqueous electrolytes,[26] the atomic concentration of fluorine (13%) is considerably increased using the organic electrolyte. However, the fluorine concentration is dramatically reduced in the annealed samples, to 1.6%; GAXRD gives no indication of TiO_xF_y or TiO_xS_y in the samples. Hence, while the results of XPS and XRD indicate a considerable amount of solvent is trapped in the amorphous anodic films, the trapped elements such as F, C, and S do not enter the rutile or anatase lattice.

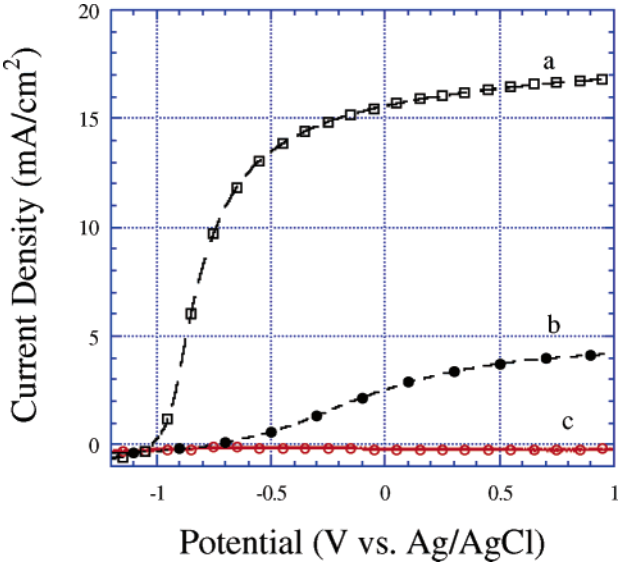

Figure 7. Photocurrent density versus applied potential (vs Ag/AgCl) in 1 M KOH solution under UV (320−400 nm) illumination (96 mW/cm^2). Anodic samples prepared as follows: **(a)** titanium foil anodized at 20 V for 70 h in DSMO and ethanol mixture solution (1:1) containing 4% HF; **(b)** H_2O−HF electrolyte at 20 V for 1 h. Both samples were annealed at 550 °C for 6 h in oxygen atmosphere prior to testing. Dark current for each sample is shown in c.

Photoelectrochemical Characteristics of TiO_2 Nanotubes Obtained in Organic Electrolytes. Our interest lies in shifting the band gap of the TiO_2 nanotube arrays to enhance their visible spectrum response for efficient solar production of hydrogen by water photolysis. It is worthy to note that the amorphous titania nanotube arrays have no discernible photoresponse under either UV or visible spectrum illumination, consequently it is necessary to crystallize the samples by annealing prior to conducting photoelectrochemical measurements. The photocurrent density (linear sweep voltammetry) of TiO_2 nanotube-array electrodes in 1 M KOH solution as a function of applied potential under UV illumination are shown in Figure 7. The short-circuit photocurrent density of the sample anodized in 1:1 DMSO and ethanol containing 4% HF solution, Figure 7, curve a, is more than six times the value for the sample obtained in a 1% hydrofluoric acid aqueous solution, Figure 7, curve b. Furthermore the slope of the photocurrent−potential curve is significantly enhanced in the organic electrolyte sample. The observed dark current for both samples was found to be negligible; see Figure 7, curve c.

The enhanced photoresponse of the sample anodized in DMSO and ethanol may be due to the distinct tube structure. Nanotube arrays obtained in a 1% hydrofluoric acid aqueous solution are approximately 500 nm in length,[4] which is much shorter than the nanotubes obtained in the organic electrolyte. We hypothesize that the longer TiO_2 nanotubes are more efficient at light trapping than their shorter counterparts, which in turn results in enhanced photoconversion efficiency. Furthermore the variation in nanotube length within the array, seen

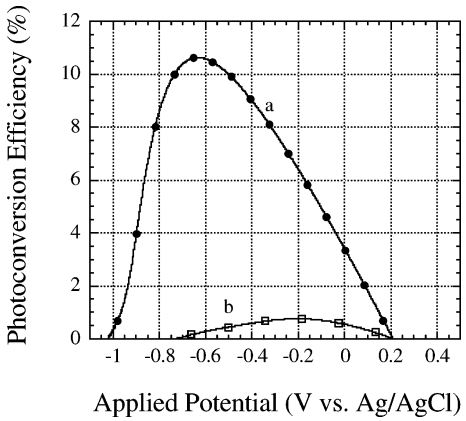

Figure 8. Photoconversion efficiency as a function of applied potential (V vs Ag/AgCl) in 1 M KOH solution for the sample prepared at 20 V in **(a)** an electrolyte of DSMO and ethanol mixture solution (1:1) containing 4% HF. **(b)** Sample anodized in H_2O-HF at 20 V for 1 h. Both samples were annealed at 550 °C for 6 h in oxygen atmosphere.

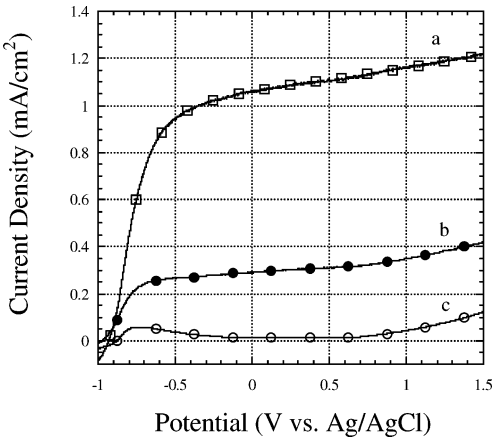

Figure 9. Variation of visible photocurrent density versus potential (vs Ag/AgCl) in 1 M KOH solution under AM 1.5 illumination (100 mW/cm^2). Anodic samples prepared as **(a)** titanium foil anodized at 20 V for 70 h in DSMO and ethanol mixture solution (1:1) containing 4% HF. (b) H_2O-HF electrolyte at 20 V for 1 h. Both samples were annealed at 550 °C for 6 h in oxygen atmosphere prior to testing. Dark current for each sample is shown in c.

clearly in Figure 3, results in a larger effective surface area in close proximity with the electrolyte, thus enabling diffusive transport of photogenerated holes to OH^- in the electrolyte to generate oxygen in a water-splitting reaction. For photoelectrodes with large semiconductor/electrolyte interface surface areas, minority carriers generated within a distance from the surface equal to the sum of the width of the depletion layer and the diffusion length escape recombination, reaching the electrolyte contact to do useful work.[28,29]

The photoconversion efficiency η of light energy to chemical energy in the presence of an external applied potential is calculated:[30]

$$\eta\ (\%) = [(\text{total power output} - \text{external applied electrical power input})]/[\text{light power input}] \times 100$$

$$\eta\ (\%) = j_p[(E^0_{rev} - |E_{app}|)/I_0] \times 100$$

The photocurrent density j_p is in mA/cm^2, the total power output is $j_pE^0_{rev}$, and the external applied electrical power input is $j_p|E_{app}|$. The term E^0_{rev} is the standard reversible potential which is 1.23 V NHE^{-1}. $E_{app} = E_{meas} - E_{ocp}$, the term E_{meas} is the electrode potential (vs Ag/AgCl) of the working electrode at which the photocurrent was measured under illumination, and E_{ocp} is the electrode potential (vs Ag/AgCl) of the same working electrode at open circuit under the same illumination and in the same electrolyte. I_0 is the intensity of incident light in mW/cm^2.

The photoconversion efficiency as a function of applied potential for the photoanode prepared in 1:1 DMSO and ethanol containing 4% HF electrolyte is shown in Figure 8. A maximum photoconversion efficiency of 10.7% is obtained for nanotubes anodized in the DMSO containing organic electrolyte. This is, to our knowledge, the second highest reported photoconversion efficiency for a titania based photoelectrochemical cell; a photoconversion efficiency of 12.8% being reported for 6.0 μm long titania nanotube arrays made using a KF based electrolyte.[30] The maximum photoconversion efficiency for the sample obtained in the organic electrolyte is a factor of 14 times greater than that obtained in the HF-based aqueous solution. Figure 9 shows the photoresponse of TiO_2 nanotube-array photoanodes recorded under visible spectrum AM 1.5 illumination. The short circuit photocurrent density of the sample anodized in organic electrolyte, curve a, is approximately four times the value for the sample obtained in aqueous solution, curve b. However, the short-circuit photocurrent density of the organic sample under visible spectrum, AM 1.5, illumination is only 7% of that under UV irradiation.

Conclusions

We have investigated in detail the electrochemical anodization of titanium in an organic electrolyte containing 4% HF, resulting in a highly ordered titania nanotube array with a unique surface morphology. Electrolyte solvents were found to reside within the as-fabricated anodic films, which were subsequently removed by annealing. The structure, morphology, and photoelectrochemical properties were studied in comparison to the nanotube arrays fabricated using a 1% HF electrolyte.[4] We conclude that titania nanotube arrays with improved photochemical response can be obtained using electrochemical anodization of titanium in fluorinated organic electrolytes by optimizing etching time, applied potential, solvents, and the HF concentration. This work opens a new way to engineer titanium dioxide nanostructures.

References and Notes

(1) Varghese, O. K.; Gong, D. W.; Paulose, M.; Ong, K. G.; Dickey, E. C.; Grimes, C. A. Extreme changes in the electrical resistance of titania nanotubes with hydrogen exposure. *Adv. Mater.* **2003**, *15*, 624−627.

(2) Livraghi, S.; Votta, A.; Paganini, M. C.; Giamello, E. The nature of papamagnetic species in nitrogen doped TiO_2 active in visible light photocatalysis. *Chem. Commun.* **2005**, *4*, 498−500.

(3) Hagfeldt, A.; Gratzel, M. Molecular photovoltaics. *Acc. Chem. Res.* **2000**, *33*, 269−277.

(4) Gong, D. W.; Grimes, C. A.; Varghese, O. K. Titanium oxide nanotube arrays prepared by anodic oxidation. *J. Mater. Res.* **2001**, *16*, 331−334.

(5) Choi, J.; Wehrspohn, R. B.; Lee, F.; Gösele, U. Anodization of nanoimprinted titanium: A comparison with formation of porous alumina. *Electrochim. Acta* **2004**, *49*, 2645−2652.

(6) Chu, S. Z.; Inoue, S.; Wada, K.; Hishita, S.; Kurashima, K. A new electrochemical lithography: Fabrication of self-organized titania nanostructures on glass by combined anodization. *J. Electrochem. Soc.* **2005**, *152*, B116−B124.

(7) Masuda, H.; Kanezawa, K.; Nakao, M.; Yokoo, A. Tamamura, T.; Sugiura, T.; Minoura, H.; Nishio, K. Ordered arrays of nanopillars formed by photoelectrochemical etching on directly imprinted TiO_2 single crystals. *Adv. Mater.* **2003**, *15*, 159−161.

(8) Wijnhoven, J. E.; Vos, W. Preparation of photonic crystals made of air spheres in titania. *Science* **1998**, *281*, 802−804.

(9) Wang, W. Z.; Varghese, O. K.; Paulose, M.; Grimes, C. A. A study on the growth and stucture of titania nanotubes. *J. Mater. Res*. **2004**, *19*, 417−422.

(10) Bavykin, D. V.; Parmon, V. N.; Lapkin, A. A.; Walsh, F. C. The effect of hydrothermal conditions on the Mesoporous structure of TiO_2 nanotubes. *J. Mater. Chem*. **2004**, *14*, 3370−3377.

(11) Chen, P. L.; Kuo, C. T.; Pan, F. M. Preparation and phase transformation of highly ordered TiO_2 nanodot arrays on sapphire substrates. *Appl. Phys. Lett*. **2004**, *84*, 3888−3890.

(12) Hoyer, P. Formation of a titanium dioxide nanotube array. *Langmuir* **1996**, *12*, 1411−1413.

(13) Li, X. H.; Liu, W. M.; Li, H. L. Template synthesis of well-aligned titanium dioxide nanotubes. *Appl. Phys. A* **2005**, *80*, 317−320.

(14) Beranek, R.; Hildebrand, H.; Schmuki, P. Self-organized porous titanium oxide prepared in H_2SO_4/HF electrolytes. *Electrochem. Solid-State Lett*. **2003**, *6*, B12−B14.

(15) Zwilling, V.; Darque-Ceretti, E.; Boutry-Forveille, A.; David, D.; Perrin, M. Y.; Aucouturier, M. Structure and physicochemistry of anodic oxide filmes on titanium and TA6V alloy. *Surf. Interface Anal*. **1999**, *27*, 629−637.

(16) Cai, Q. Y.; Paulose, M.; Varghese, O. K.; Grimes, C. A. The effect of electrolyte composition on the fabrication of self-organized titanium oxide nanotube arrays by anodic oxidation. *J. Mater. Res*. **2005**, *20*, 230−234.

(17) Propst, E. K.; Kohl, P. A. The electrochemical oxidation of silicon and formation of porous silicon in acetonitrile. *J. Electrochem. Soc*. **1994**, *141*, 1006−1013.

(18) Christophersen, M.; Carstensen, J.; Föll, H. Crystal orientation dependence of macropore formation in p-type silicon using organic electrolytes. *Phys. Status Solidi* A **2000**, *182*, 103−107.

(19) Christophersen, M.; Carstensen, J.; Voigt, K.; Föll, H. Organic and aqueous electrolytes used for etching macro- and mesoporous silicon. *Phys. Status Solidi A* **2003**, *197*, 34−38.

(20) Ponomarev, E. A.; Levy-Clement, C. Macropore formation on p-type Si in fluoride containing organic electrolytes. *Electrochem. Solid-State Lett*. **1998**, *1*, 42−45.

(21) Föll, H.; Christophersen, M.; Carstensen, J.; Hasse, G. Formation and application of porous silicon. *Mater. Sci. Eng. R* **2002**, *39*, 93−141.

(22) Liu, Y.; Alwitt, R. S.; Shimizu, K. Cellular porous anodic alumina grown in neutral organic electrolyte. I. Structure, composition, and properties of the films. *J. Electrochem. Soc*. **2000**, *147*, 1382−1387.

(23) Casillas, N.; Charlebois, S.; Smyrl, W. H. *J. Electrochem. Soc*. **1994**, *141*, 636.

(24) Archibald, L. C.; Leach, J. S. L. *Electrochim. Acta* **1977**, *22*, 21.

(25) Lorenzo de Mele, M. F.; Cortizo, M.C. *J. Appl. Electrochem*. **2000**, *30*, 95−100.

(26) Ruan, C.; Paulose, M.; Varghese, O. K.; Grimes, C. A. *J. Nanosci. Nanotechnol.*, submitted for publication.

(27) Astrova, E. V.; Borovinskaya, T. N.; Tkachenko, A. V.; Balakrishnan, S.; Perova, T. S.; Rafferty, A.; Gun'ko, Y. K. *J. Micromech. Microeng*. **2004**, *14*, 1002−1028.

(28) Sukamto, J. P. H.; Smyrl, W. H.; Mcmillan, C. S.; Kozlowski, M. R. *J. Electrochem. Soc*. **1992**, *38*, 15−27.

(29) Van de Lagemaat, J.; Plakman, M.; Vanmaekelbergh, D.; Kelly, J. *J. Appl. Phys. Lett*. **1996**, *69*, 2246−2248.

(30) Varghese, O. K.; Paulose, M.; Shankar, K.; Mor, G. K.; Grimes, C. A. *J. Nanosci. Nanotechnol*. **2005**, *5*, 1158−1165.